

## Supplementary Methods

### ***Network Coherence Analyses***

#### *Mean Network Coherence Coefficient*

For each participant, the network coherence coefficient was calculated by taking the average regression coefficient across voxels for each back-transformed ICN map as follows. The participant-level maps were generated as the second stage of FSL's dual regression algorithm. First, the group-level component map was used as a spatial regressor in a general linear model (GLM) to determine participant-level component timecourses using each individual's preprocessed functional data. In the second stage, the values in the map resulted from using each participant's ICN timecourse as a temporal regressor for all brain voxels. Hence, these regression coefficient values represented how well each voxel cohered to that ICN's timecourse for that individual. Each map was then thresholded at  $z=6$  and the `fslmaths` tool was used to compute the average across voxels within that thresholded mask. Hence, the resulting mean coherence values were a measure of intra-network coherence and can be used for individual difference measures, as well as cross-task consistency and familiarity as in this case.

#### *Voxel-wise Network Coherence Coefficient*

Similarly, the reliability of intra-network coherence between twins was assessed at the voxel-level using the intraclass correlation formula defined in Wisner et al. (2013). Hence ICC's were calculated between twins for all voxels (rather than the average) within a given component. These voxel-level, twin-pair ICC's were then averaged per ICN to determine the voxel-wise familiarity of each ICN.

### ***Anatomical Similarity of Brains after Co-Registration***

#### *Spatial Overlap of High Resolution Structural Brain Scans*

In order to address the possible genetic contribution of anatomical similarity and structural covariance to the generation of the ICNs and the subsequent heritability estimates, Spearman correlations and Dice similarity calculations were performed on the T1 structural maps for all individuals after co-registration to the MNI 2mm brain using FSL's FLIRT algorithm. The subsets of scores for twin pairs and pairs of non-related individuals were then assessed for group differences using a non-parametric permutation test.

#### *Spatial Overlap of High Resolution Structural Brain Scans*

It was pertinent to also assess the covariance of the spatial features of the actual functional data that was being input into the initial group ICA and dual regression algorithms to assess whether this covariance was higher for twins. Hence, an analogous Spearman correlation and permutation test procedure was performed on the functional scans after registration to the high-resolution scans and then the MNI 2mm brain.

### ***Consistency of Head Movements***

Another analysis was done to address the potential confound of head motion being more similar between twins than among unrelated participants and this motion correlation having an impact on networks generated via ICA in the two tasks. First, a root mean square displacement vector was calculated per individual from the six motion parameters measured using FSL's MCFLIRT algorithm which included estimates of translation in the

three axes as well as roll, pitch and yaw rotations. Similar to the structural covariance metric, Spearman correlations were performed between the displacement vectors for all individuals and a permutation test was used to determine if there were group differences between twin scores and those of unrelated individuals.

Another concern was whether motion was influencing and/or inflating the ICN timecourses and the estimates of task-relatedness or timecourse familiarity. Hence, an additional intraclass correlation calculation was performed between the motion displacement vector and ICN timecourses per individual. These ICC's were then averaged to determine the overall influence of motion on each of the ICNs.

### ***Significance Testing***

The significance thresholds for the inference correlations and the relationship to task correlations were established using t-tests of the transformed 'r' values with effective sample sizes. This is due to the fact that the monozygotic twins share an amount of genetic variance that could possibly violate the assumption of independence in the t-test and, hence, this was addressed by adjusting the estimates using the effective sample size (Pedlow, Wang, & Muirheartaigh, 2005; Yaning Yang et al., 2011). Statistical significance for the spatial familiarity metric, the coherence familiarity metric, and the task HRF familiarity metric were established using t-tests of the transformed values, which provided p-values and confidence intervals. For the spatial familiarity metric, a t-transform of the Spearman rho values was used for significance testing. For the coherence familiarity metric, the ICC test that was performed provided p-values and confidence intervals (Revelle, 2011). For the task HRF familiarity metric, the Pearson's 'r' correlation values were tested using a

one-sample t-test of the transformed values. Finally, due to the fact that a t-test was performed per network, Bonferroni corrections for multiple comparisons were performed after significance testing in order to address the possibility of family-wise errors and to establish corrected significance thresholds.

### ***3D Brain Figure Generation***

All brain images were generated using Mango (the Multi-image Analysis GUI) viewer from the Research Imaging Institute of University of Texas Health Science Center (<http://ric.uthscsa.edu/mango/index.html>). All ICN overlays from the group-level ICA output were rendered on a 3D surface build of the MNI 152 T1 1-mm brain template. This 3D rendering was then made to be translucent in order to reveal the subsurface structures contained in each ICN. This was particularly important for sub-cortical structures such as the basal ganglia network or subgenual OFC & ACC network.

## Supplementary Results

### ***Anatomical Similarity of Brains after Co-Registration***

#### *Spatial Overlap of High Resolution Structural Brain Scans*

The non-parametric permutation test revealed no observable differences between twin scores and non-twin scores after registration to the MNI 2mm standard brain. Hence, whatever genetic contribution there was to the anatomy of the twins' brains, that

contribution was efficiently removed by the linear transformation into standard space and, consequently, the overlap of each brain with the standard MNI template was not heritable.

#### *Spatial Overlap of High Resolution Structural Brain Scans*

After calculating the spatial Spearman correlation of transformed mean functional maps, these scores were not found to be familial using a permutation procedure. Hence, the process of co-registration of the functional data to the high resolution anatomical scans and then the standard brain template eliminated any possible contribution of structural similarities (Supplementary Figure 3a).

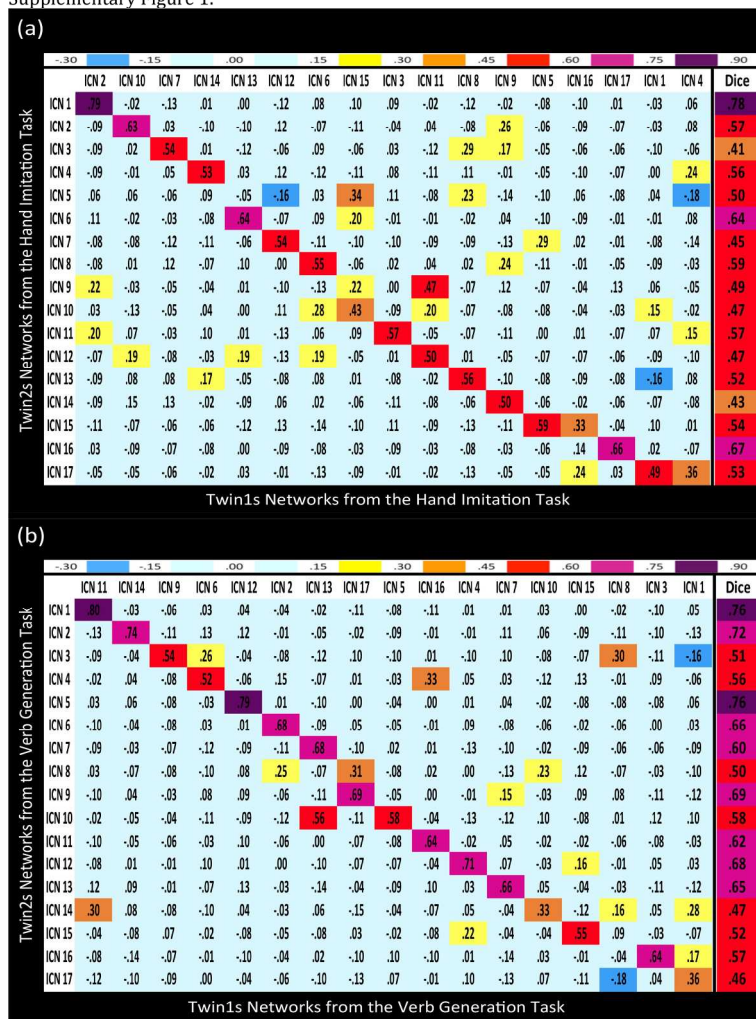
#### ***Consistency of Head Movements***

No differences in movement were found between twins versus non-twins and, hence, motion was not heritable. In addition, the intraclass correlations between motion displacement and ICN timecourses were essentially zero across the board and this implies that motion did not influence the ICN timecourses in any way (Supplementary Figure 3b). These results are not surprising since temporal filtering is one of the preprocessing steps and artifactual ICA components related to respiration and other movements were previously identified and removed.

**Supplementary Figure 1.** Spearman rank-order correlations and Dice similarity correlations were calculated between ICN maps from an ICA of data from the first twin from each twin pair (Twin 1s) and the ICN maps from an ICA of data from the second twin from each twin pair (Twin 2s). These correlations were performed for data from both (a) the hand imitation task and (b) the verb generation task. The two sets of ICA-derived ICNs were assessed for having at least a modest score on the Dice similarity index ( $s \geq 0.4$ ). In addition, the Spearman correlations were found to be significant above a threshold of ( $r \geq 0.433$ ).

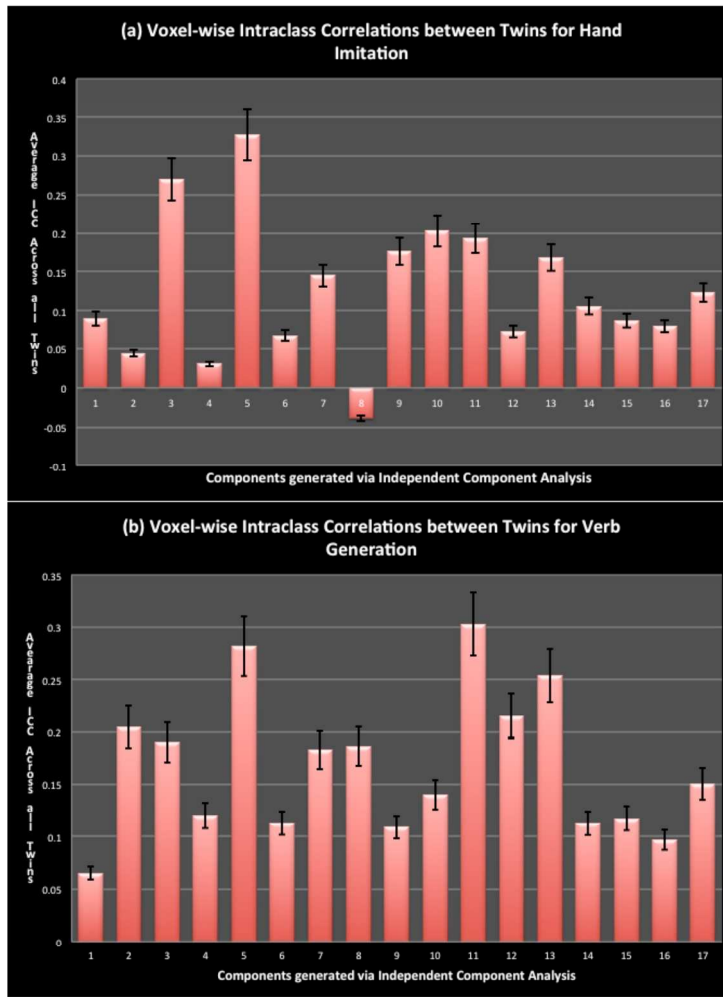
**Supplementary Figure 2.** Participant-level ICN spatial maps were first masked using a binarized image of the corresponding group-level map that had been pre-thresholded at  $z = 6$ . All of the voxelwise ICC computations for (a) hand imitation and (b) verb generation were performed using algorithms constructed with the fslmaths tool. (<http://www.fmrib.ox.ac.uk/fslcourse/lectures/practicals/intro/index.htm>)

Supplementary Figure 1.



260x358mm (300 x 300 DPI)

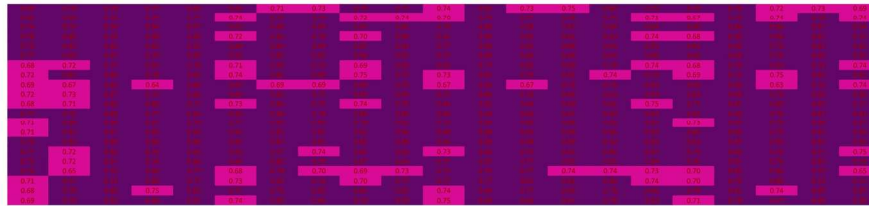
Supplementary Figure 2.



260x372mm (300 x 300 DPI)



Supplementary Figure 3a. Spearman correlation of participant functional scans after co-registration



Supplementary Figure 3b. Intraclass correlations of movement and ICN timecourses

(i) Hand Imitation

Table with 17 columns: Participant, ICN1-ICN17, and Avg per person. It contains intraclass correlation values for 42 participants across 17 independent components (ICNs) during a hand imitation task. The values range from approximately -0.15 to 0.45.

(ii) Verb Generation

214x243mm (300 x 300 DPI)

Connectivity in Monozygotic Twins 8

Participant	ICN1	ICN2	ICN3	ICN4	ICN5	ICN6	ICN7	ICN8	ICN9	ICN10	ICN11	ICN12	ICN13	ICN14	ICN15	ICN16	ICN17	ICN18	Avg per person
1	-1.05E-06	3.95E-07	-1.89E-07	-1.13E-06	-3.90E-09	-6.44E-07	-1.43E-06	-9.91E-07	-6.35E-07	5.01E-08	-8.78E-07	-3.35E-07	2.32E-08	-5.58E-07	7.81E-07	-3.50E-07	-6.52E-07	-9.57E-07	-4.52E-07
2	-2.27E-06	-3.73E-06	-6.45E-07	-2.54E-06	4.51E-06	-2.57E-06	2.44E-06	-6.62E-07	1.90E-06	-1.19E-06	-1.05E-06	-2.95E-07	1.77E-07	-2.04E-06	-1.93E-06	-6.80E-06	-2.86E-06	-1.67E-07	-8.11E-04
3	5.71E-07	-1.89E-07	-1.04E-07	-1.59E-06	2.99E-06	1.10E-06	-2.30E-07	-4.42E-07	1.29E-08	-1.13E-07	-5.28E-07	-4.86E-07	-3.43E-07	-1.46E-07	-8.08E-07	4.98E-08	6.81E-07	-1.67E-05	-8.27E-07
4	-4.29E-07	-1.77E-06	-7.89E-06	-3.34E-06	-3.77E-06	-1.79E-06	1.75E-06	4.86E-06	2.62E-06	-3.72E-06	6.82E-07	1.82E-06	-1.60E-06	-1.69E-06	4.52E-06	7.14E-06	-8.08E-06	6.73E-05	2.22E-06
5	-5.82E-06	-5.49E-07	3.88E-06	2.78E-06	-7.74E-07	4.11E-06	3.22E-06	7.72E-06	1.54E-06	3.98E-06	-7.30E-06	-2.40E-06	1.50E-06	2.37E-06	-6.19E-07	6.31E-06	-1.80E-06	1.45E-04	8.96E-06
6	-1.92E-06	1.36E-06	8.81E-07	-2.21E-06	-1.04E-05	-3.71E-07	2.90E-08	3.27E-06	-1.75E-06	8.19E-07	-3.30E-06	-1.57E-06	1.51E-07	-4.71E-07	8.73E-07	-8.58E-07	-3.25E-06	3.51E-05	7.64E-07
7	1.00E-07	-1.97E-07	7.51E-08	-2.85E-07	4.93E-07	-5.10E-07	-3.61E-09	2.63E-07	1.11E-07	-1.32E-07	-1.36E-07	-3.61E-08	5.28E-08	-1.08E-08	-8.55E-08	2.68E-07	-2.34E-07	6.48E-06	3.48E-07
8	-3.73E-07	1.58E-07	7.98E-07	1.97E-07	-3.41E-06	-8.59E-07	2.21E-07	4.74E-07	-6.23E-07	1.53E-06	-2.54E-08	-8.68E-08	3.15E-07	-8.99E-08	2.97E-06	4.88E-07	-6.03E-07	3.87E-05	2.20E-06
9	-4.70E-07	1.42E-06	7.82E-07	3.95E-06	2.88E-06	-1.13E-06	4.83E-06	-1.07E-05	-5.22E-07	5.28E-07	1.19E-06	-1.98E-07	-1.46E-06	-1.50E-06	8.71E-07	-1.23E-05	-7.44E-06	-1.38E-06	1.25E-06
10	-1.66E-07	-1.21E-07	6.09E-08	-3.18E-07	-2.04E-06	-8.98E-08	-1.41E-07	6.98E-07	-5.44E-07	-1.61E-08	-1.81E-07	-5.59E-09	7.13E-08	2.47E-07	-1.61E-07	9.28E-07	-1.80E-06	8.73E-05	-3.54E-06
11	-2.38E-06	9.24E-08	2.21E-06	-2.13E-07	-1.13E-05	-1.57E-06	2.16E-06	2.54E-06	-2.82E-06	4.41E-06	6.69E-08	1.84E-06	-3.44E-07	7.84E-07	8.80E-07	5.41E-07	-7.80E-06	2.84E-03	1.11E-04
12	-3.44E-06	4.85E-07	-3.70E-06	-5.80E-07	-8.53E-06	-3.30E-06	-6.51E-07	3.87E-06	-3.05E-06	2.27E-07	-1.17E-06	-3.61E-06	-1.20E-06	-8.79E-07	-1.63E-06	-8.08E-07	-1.09E-05	-2.98E-05	-3.77E-06
13	-1.14E-05	8.45E-06	1.00E-06	7.99E-06	-1.73E-05	5.78E-07	-1.56E-06	-5.58E-06	-5.11E-06	4.64E-07	2.12E-06	2.69E-07	6.44E-07	7.81E-06	-5.56E-05	-2.29E-05	-4.86E-05	-6.81E-06	-6.81E-06
14	6.82E-07	9.81E-07	4.66E-07	2.25E-06	7.88E-06	1.33E-06	9.82E-07	5.08E-06	2.42E-06	1.89E-06	1.17E-06	1.25E-06	9.11E-07	-2.79E-06	-1.86E-06	8.49E-06	7.08E-07	1.17E-04	1.17E-04
15	-1.86E-07	4.14E-07	-3.97E-07	-3.13E-07	-1.51E-06	-1.64E-07	2.72E-09	-1.81E-07	-5.74E-07	-3.24E-07	-2.85E-08	-8.88E-08	-2.07E-08	-1.26E-07	-7.11E-07	3.67E-07	-1.46E-06	1.04E-07	5.24E-05
16	-4.09E-06	-4.88E-07	-2.11E-06	5.73E-06	-4.13E-06	-8.61E-08	-8.42E-06	-2.22E-06	-3.51E-06	-1.22E-06	4.85E-07	-3.01E-08	8.01E-07	-1.46E-06	6.48E-06	-3.17E-06	-5.58E-06	-1.47E-04	-9.83E-06
17	-5.37E-07	-1.18E-07	-2.12E-07	2.11E-06	2.34E-06	3.32E-09	-1.04E-06	8.75E-07	-3.21E-07	-8.45E-08	-5.22E-07	-7.42E-07	-9.74E-07	-4.02E-08	-2.22E-07	-1.99E-07	-3.16E-07	1.65E-05	8.26E-07
18	-1.45E-05	-2.44E-06	3.43E-06	-8.14E-06	-2.03E-05	-1.88E-06	1.50E-05	6.57E-06	-1.28E-05	9.65E-06	-5.54E-06	-1.11E-05	-8.34E-06	1.24E-06	-1.12E-05	-1.42E-06	5.42E-06	2.92E-05	-1.50E-06
19	2.55E-07	-1.38E-07	-1.55E-07	-2.08E-07	6.07E-07	-7.16E-08	3.38E-07	7.21E-08	2.18E-07	-2.08E-07	4.07E-08	6.81E-08	-1.37E-07	-1.17E-07	-5.49E-07	-2.15E-07	1.65E-07	2.21E-05	1.20E-06
20	-2.15E-07	4.44E-08	-5.58E-08	6.94E-08	3.14E-07	2.78E-08	-1.37E-07	-1.44E-06	-3.61E-08	-1.06E-07	2.42E-08	-4.52E-07	-1.92E-07	-1.78E-07	-3.57E-07	9.10E-07	-1.53E-06	6.38E-07	-1.48E-07
21	-1.99E-07	6.01E-07	3.80E-07	5.86E-07	2.62E-07	1.13E-06	-5.43E-07	-1.21E-07	6.75E-07	-2.13E-07	4.89E-07	5.55E-07	1.17E-07	-9.11E-09	4.81E-06	-8.64E-05	-1.18E-05	-8.01E-06	-5.48E-06
22	6.51E-09	-5.99E-08	-6.93E-08	2.11E-07	2.75E-07	3.62E-10	-3.51E-08	1.28E-07	1.34E-07	-1.12E-08	1.52E-07	4.64E-08	1.72E-07	-3.80E-08	-3.91E-07	-6.71E-07	2.99E-07	-2.17E-06	-2.00E-07
23	-5.57E-05	-3.57E-05	-6.23E-07	-4.30E-06	-1.24E-04	-6.48E-05	-4.61E-05	-2.80E-05	-3.66E-06	-2.68E-05	-1.24E-05	4.71E-06	-3.11E-05	-3.73E-05	-2.88E-05	-5.48E-05	-1.89E-05	2.00E-05	-3.23E-05
24	1.06E-06	-1.69E-06	-8.78E-08	4.97E-07	2.71E-06	8.10E-07	4.61E-07	4.14E-07	1.24E-06	3.67E-07	-6.80E-07	-1.01E-06	8.79E-07	-1.97E-07	1.97E-06	-3.77E-07	-1.34E-06	-1.84E-05	-8.68E-07
25	3.96E-06	4.01E-07	-1.22E-06	-1.33E-06	4.39E-06	7.48E-07	-7.92E-06	-3.89E-06	1.81E-06	-2.42E-06	-4.89E-07	-4.14E-07	1.07E-06	-1.10E-06	-7.19E-07	-2.35E-07	-2.61E-06	-4.38E-04	-2.49E-05
26	-5.18E-06	-6.76E-06	-2.11E-06	2.99E-06	-2.07E-06	-1.92E-05	-1.14E-05	-1.41E-05	-5.84E-06	-7.44E-07	-8.76E-06	-5.73E-06	-2.67E-06	-3.42E-06	3.50E-06	-1.50E-05	4.73E-05	-2.03E-04	-1.93E-05
27	-1.57E-07	2.33E-07	1.14E-07	1.60E-07	-1.59E-06	-3.50E-07	1.84E-08	5.71E-07	4.48E-09	1.07E-07	-6.53E-08	2.66E-08	7.45E-08	8.99E-08	3.45E-07	2.74E-07	-3.65E-07	1.03E-07	5.73E-05
28	-2.17E-07	6.31E-08	2.19E-07	6.80E-07	-4.18E-06	-8.21E-08	-3.52E-07	1.35E-07	-6.83E-07	3.29E-07	-7.99E-08	2.81E-08	-6.43E-08	2.39E-07	1.80E-06	-1.65E-07	-5.78E-07	-9.54E-06	-7.23E-07
29	8.49E-08	1.45E-07	7.90E-08	1.50E-07	5.11E-07	-5.10E-07	-3.72E-07	4.58E-08	2.40E-07	4.58E-08	-2.58E-08	4.77E-08	-4.40E-09	4.61E-07	4.75E-08	-3.65E-07	9.46E-06	5.57E-07	5.57E-07
30	-4.29E-07	5.04E-08	-3.20E-07	-1.41E-07	-1.40E-06	1.38E-07	1.33E-07	4.72E-07	-4.32E-07	2.63E-08	-3.23E-07	-5.95E-07	-1.30E-07	-2.74E-07	1.39E-07	-4.67E-07	-2.25E-06	1.31E-05	4.00E-07
31	1.03E-06	6.02E-08	-1.65E-06	1.01E-06	2.04E-06	1.61E-07	-1.28E-06	-1.19E-06	1.86E-06	-1.18E-06	3.64E-07	-2.70E-07	1.42E-06	2.31E-06	-7.96E-07	1.14E-06	-1.54E-07	-6.76E-07	-6.76E-07
32	7.24E-07	-1.05E-06	-7.83E-07	2.12E-06	-5.04E-07	3.60E-06	-4.05E-07	-9.47E-07	2.33E-06	-2.35E-06	6.35E-07	1.41E-06	4.75E-07	9.88E-07	4.66E-06	5.61E-06	9.84E-07	-4.54E-06	7.21E-07
33	-5.13E-07	3.90E-08	3.20E-08	-2.13E-07	-2.02E-06	-8.41E-07	7.17E-07	-1.65E-07	-5.99E-07	4.05E-07	-1.18E-07	-4.71E-08	-2.54E-07	1.61E-08	-1.74E-08	-1.07E-06	-1.09E-06	1.81E-04	1.02E-04
34	5.51E-07	-2.29E-07	6.70E-07	-2.29E-08	-1.11E-06	-2.05E-06	3.23E-07	1.26E-06	-4.67E-07	1.64E-06	-1.63E-07	1.18E-07	-2.52E-07	1.04E-07	-2.60E-07	6.39E-06	-5.27E-06	1.39E-05	7.79E-07
35	3.15E-07	4.66E-07	-3.01E-06	-1.28E-06	2.76E-06	2.20E-06	-7.55E-07	-8.77E-08	9.68E-07	-6.47E-07	-3.08E-07	5.51E-08	-2.28E-07	-2.52E-07	4.22E-07	-2.88E-06	-1.12E-06	-1.00E-04	-5.78E-06
36	7.18E-07	-1.11E-07	-1.44E-07	-4.67E-07	5.05E-07	-4.80E-07	3.96E-07	-6.12E-07	2.71E-07	5.14E-08	-9.74E-08	-7.54E-08	-5.24E-07	-3.11E-07	3.21E-07	8.88E-08	8.40E-08	4.49E-07	4.49E-07
37	9.84E-07	-2.28E-07	1.01E-06	2.02E-07	-3.51E-06	-5.16E-07	-3.39E-07	5.07E-06	-1.00E-06	6.82E-07	-5.36E-07	-3.09E-07	2.78E-07	-8.18E-08	8.50E-07	7.03E-07	3.42E-06	2.84E-05	1.49E-06
38	-1.15E-06	2.10E-07	3.19E-07	-6.43E-07	-4.31E-06	-1.22E-06	-3.17E-07	-1.52E-06	-1.84E-06	8.15E-08	-3.87E-07	-2.21E-07	-6.56E-07	6.29E-07	3.32E-07	2.25E-06	-1.31E-06	5.14E-05	2.25E-06
39	-3.36E-07	6.03E-07	-1.11E-07	-3.51E-07	-6.37E-07	7.81E-07	-7.19E-07	1.17E-06	-9.93E-07	5.51E-07	-6.41E-07	-8.21E-07	-8.39E-07	-2.12E-07	-9.51E-07	-1.19E-06	5.21E-06	-1.04E-04	-5.98E-06
40	1.65E-07	-2.66E-07	-1.27E-07	-4.91E-07	3.87E-07	-4.45E-07	-9.24E-07	1.64E-06	9.82E-08	-4.51E-07	4.01E-07	-2.91E-07	3.65E-08	-3.84E-07	-1.40E-07	-5.66E-07	-1.66E-06	-2.08E-03	-1.16E-04
41	2.36E-06	4.50E-07	-2.68E-06	2.39E-06	1.20E-06	4.04E-06	1.03E-05	7.98E-06	-2.34E-06	5.55E-07	2.95E-07	1.34E-06	4.95E-07	-2.41E-06	9.42E-06	1.44E-05	-6.12E-06	-1.12E-06	2.23E-06
42	1.64E-08	2.46E-08	4.20E-07	3.57E-07	-6.27E-07	1.95E-07	1.07E-06	6.66E-07	4.15E-07	-1.44E-08	3.79E-08	1.17E-07	1.29E-07	2.07E-07	5.37E-08	4.31E-07	3.50E-07	2.35E-06	2.35E-06
Avg per ICN	-2.56E-06	-9.43E-07	-2.98E-07	1.13E-07	-4.73E-06	-2.57E-06	-1.56E-06	-3.29E-07	-4.13E-07	-6.60E-07	-9.47E-07	-5.44E-07	-9.83E-07	-1.13E-06	-3.69E-07	-4.69E-06	-3.64E-06	-2.69E-04	-1.64E-05

118x77mm (300 x 300 DPI)